Geol. Mag. **145** (*4*), *2008, pp. 570–585.* © *2008 Cambridge University Press*
doi:10.1017/S0016756808004536 *Printed in the United Kingdom*

K-richterite–olivine–phlogopite–diopside–sanidine lamproites from the Afyon volcanic province, Turkey

CÜNEYT AKAL*

Dokuz Eylül University, Engineering Faculty, Department of Geological Engineering, 35160 Buca, Izmir, Turkey

(*Received* 13 March 2007; *accepted* 31 July 2007; First published online 24 April 2008)

Abstract – Middle Miocene volcanic activity in the Afyon volcanic province (eastern part of Western Anatolia) is characterized by multistage potassic and ultrapotassic alkaline volcanic successions. The volcanism is generally related to the northward subduction of the African plate beneath the Eurasian Plate. In Afyon, the Middle Miocene volcanic products consist of melilite leucitite, tephriphonolite, trachyte, basaltic–trachyandesite, phonolite, phonotephrite, tephriphonolite and lamproite rocks. Near-surface emplacement and relatively quiescent subaerial eruptions of lamproitic magma produced different emplacement forms such as dome/plug-shaped bodies and lava flows, showing variation in volume and texture. The mineralogical constituents of the lamproites are sanidine, olivine ($77 <$ Mg no. < 81), phlogopite ($74 <$ Mg no. < 78), K-richterite, clinopyroxene ($74 <$ Mg no. < 78), with accessory apatite, calcite and opaque minerals. Afyon lamproites resemble Mediterranean-type Si-rich lamproites. Their compositional range is 50–52 wt % SiO_2, 4–8 wt % MgO, and they display a typical lamproitic affinity. Chondrite-normalized REE patterns exhibit enrichment in LREE relative to HREE ($(La/Yb)_{CN} = 15.3–17.0$). They show extreme enrichment in LILE relative to primitive mantle values and troughs of Nb and Ti. The lamproites give a range of high initial $^{87}Sr/^{86}Sr$ ratios and low $^{143}Nd/^{144}Nd$ ratios. The geochemical and isotopic characteristics suggest that lamproitic magma is derived from highly metasomatized mantle. The enrichment history may include metasomatic events related to subduction, as in other active orogenic areas of the Mediterranean.

Keywords: ultrapotassic composition, lamproite, alkaline metasomatism, Turkey, Mediterranean region.

1. Introduction

Lamproitic rocks have been the subject of intense interest because they are commonly emplaced in different tectonic environments from within-plate to destructive plate boundaries. Lamproites facilitate understanding and evaluation of complex magmatic processes, including partial melting, fractional crystallization, mantle metasomatism, and crustal contamination processes for K-rich magmas (e.g. Foley, 1992*a*,*b*; Ellam *et al.* 1989; Conticelli, 1998; Duggen *et al.* 2005). However, the location, nature and ultimate origin of ultrapotassic reservoirs is a matter of debate (e.g. Peccerillo, 1992; Murphy, Collerson & Kamber, 2002).

Si-rich Mediterranean lamproites present extreme isotopic compositions, approaching the signatures of upper crust rocks (Nelson, McCulloch & Sun, 1986; Nelson, 1992). Earlier workers explored the possibility that the extremely depleted component of the mantle source of Tertiary Mediterranean lamproites is derived from an island-arc oceanic lithosphere accreted during Mesozoic subduction–Alpine collision processes (Prelević, Foley & Cvetković, 2007; Prelević *et al.* 2005).

*E-mail: cuneyt.akal@deu.edu.tr

The Kırka–Afyon–Isparta alkaline volcanic area is a Neogene–Quaternary potassic to ultrapotassic volcanic area (e.g. Alıcı *et al.* 1998; Francalanci *et al.* 1990, 2000; Çoban & Flower, 2006) related to subduction and collision resulting from the convergence of Africa and Eurasia. Since the pioneering work of Keller & Villari (1972) and Keller (1983), it has been the most investigated alkaline province in the Kırka–Afyon–Isparta region. Recent volcanological and petrographic papers have attempted to clarify the genesis and peculiar mineralogy and geochemistry of potassic–ultrapotassic rocks in the area (e.g. Savaşçın & Oyman, 1998; Francalanci *et al.* 1990, 2000; Doglioni *et al.* 2002; Akal, 2003; Innocenti *et al.* 2005; Çoban & Flower, 2006). Limited age determinations imply that volcanism in the Kırka–Afyon–Isparta area becomes young to the south from Afyon to the Isparta locations. In the Afyon region, the ages of volcanism are scattered between 14.8 ± 0.3 and 8.6 ± 0.2Ma (Besang *et al.* 1977), whereas in the Isparta region they are between 4.7 ± 0.5 and 4.07 ± 0.2 Ma (Lefevre, Bellon & Poisson, 1983).

Previous studies (e.g. Keller & Villari, 1972; Keller, 1983; Savaşçın & Oyman, 1998; Francalanci *et al.* 1990, 2000) mainly focused on the potassic–ultrapotassic rock suites in the Kırka–Afyon–Isparta volcanic area. This paper reports new whole-rock

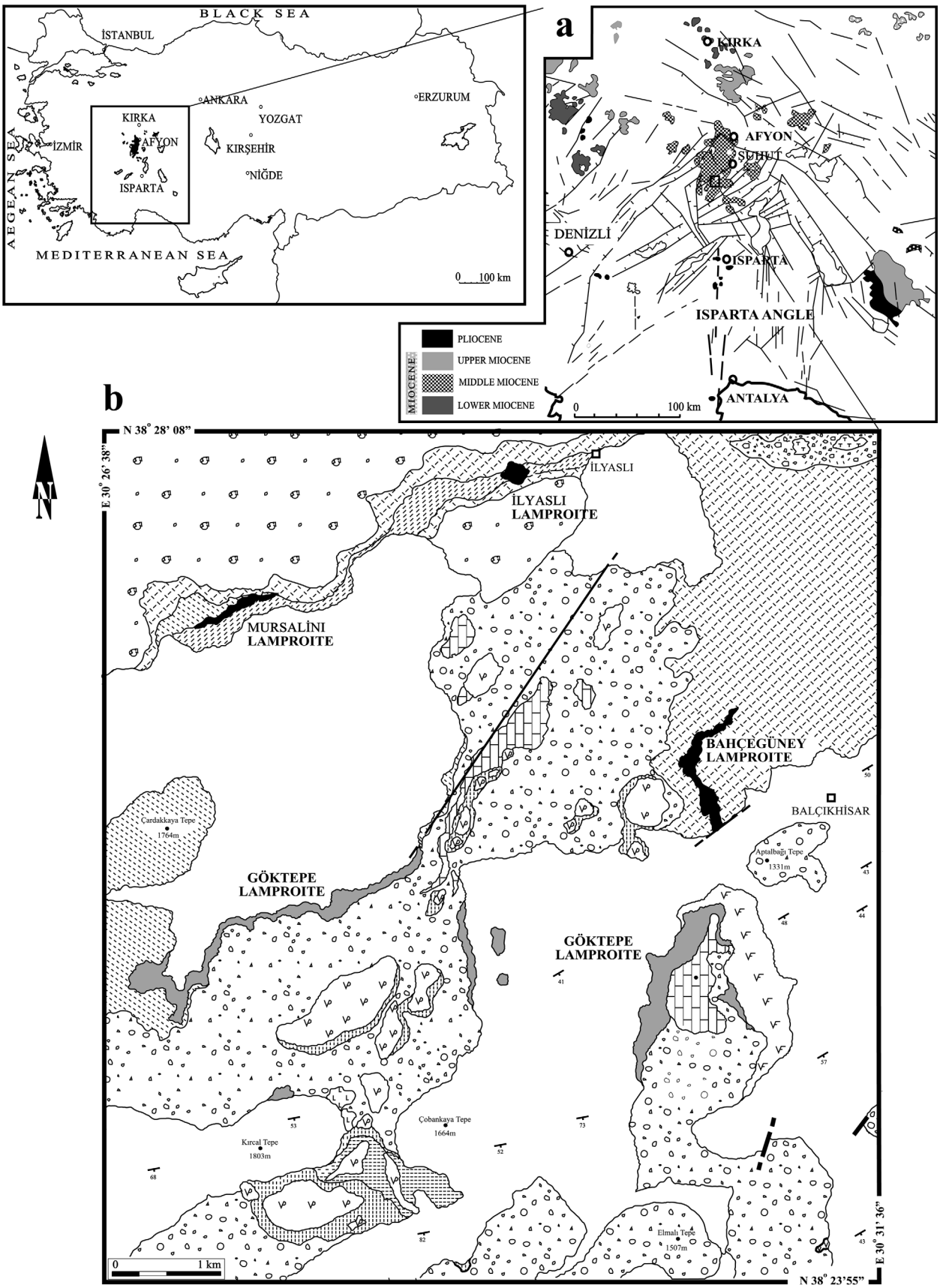

Figure 1. (a) Location map showing tectonic lines in the Western Anatolia modified from 1:500 000 scale geological map of Mineral Research and Exploration (MTA). (b) Geological map of the studied area located at the southern part of Afyon Volcanic Province. For legend see Figure 2.

https://doi.org/10.1017/S0016756808004536 Published online by Cambridge University Press

major elements, trace elements, Sr–Nd isotopic data and mineralogical compositions of lamproites in the Afyon volcanic province, to determine relationships with Mediterranean lamproites.

2. Geological setting of potassic–ultrapotassic rocks around Şuhut/Afyon

The products of Middle Miocene potassic–ultrapotassic volcanic activity overlie and intrude the sedimentary formations of the northeastern part of the western Taurides around the Şuhut/Afyon region. Based on their stratigraphic positions, the volcanic products can be divided into three groups. Melilite leucitite, tephriphonolite and voluminously small trachyandesite lavas, which had covered and intruded the sedimentary rocks of the Tauride belt, form the first group. They are mainly covered by leucitite blocks and clast-rich volcaniclastic successions and partly by lamproitic lava flows.

The second group of volcanic products is characterized by lamproitic lavas and widespread and thick trachyandesitic lavas and pyroclastic successions. Lacustrine sedimentary rocks, which are gradationally interfingered with the volcanosedimentary rocks and phonotephritic tuff, overlie both the latitic pyroclastic succession and leucitite blocks and clast-rich volcaniclastic succession. The third and last volcanic activity in the area is represented by phonotephritic lavas.

Four lamproite outcrops have been recognized near the Balçıkhisar and İlyaslı/Şuhut locations (Fig. 1). The near-surface emplacement and relatively quiescent subaerial eruptions of lamproite magma produced different emplacement forms such as lava flows and dyke-like and dome-like shapes.

2.a. İlyaslı lamproite

The İlyaslı lamproite resulted from the intrusion of a small volume of lamproitic magma into flysch facies rocks and the earlier products of trachyandesitic volcanism, such as ignimbrite and debris flows. It crystallized near the surface and/or in the subaerial environment. The outcrop is mainly covered by a latitic pyroclastic sequence.

The dome/plug-shaped lamproite body is intensely eroded and its inner structure of five concentric zones can be observed. The central part consists of a dark grey-green coarse-grained section that corresponds to the deeper facies. The middle part is composed of medium- to fine-grained grey to brownish grey rocks. The upper part presents volcanic facies characterized by reddish brown flow lamination and vesicular texture. The top of the body has an oxidized and silicified red zone.

Sanidine phenocrysts about 1 × 1 cm in diameter occur in the groundmass of the coarse-grained lavas. In the fine- to medium-grained lava, platy phlogopite

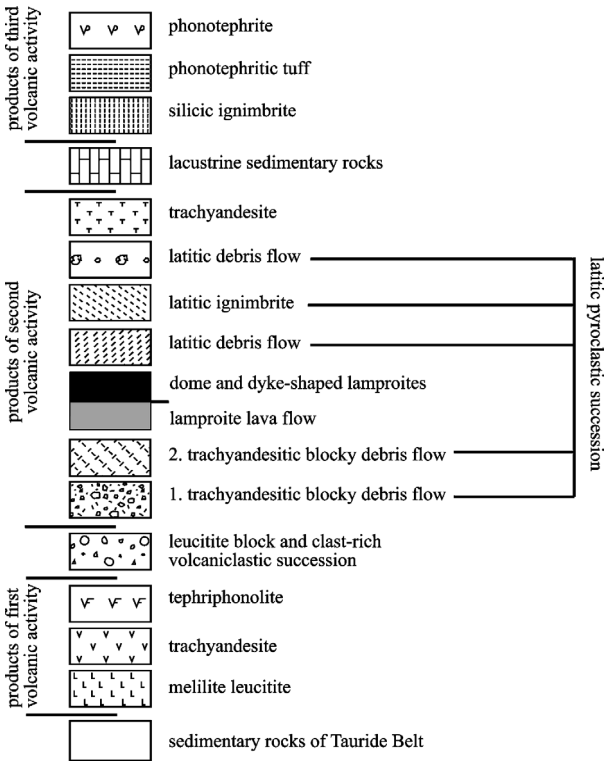

Figure 2. Simplified stratigraphy of the studied area.

phenocrysts (up to 5 mm) and olivine crystals (2–3 mm) are distinguished. Samples from the upper part of the body are rich in vesicles filled by chalcedony. In these samples, flow structure is distinguished by the presence of oriented phlogopite phenocrysts and different coloured thin flow bands.

2.b. Mursalini Lamproite

Lamproitic volcanism at the Mursalini location produced minor amounts of pyroclastic rocks followed by the emplacement of lava flows. These products overlie a trachyandesitic ignimbrite, and latitic pyroclastic successions also cover all products of lamproitic activity. The yellowish-white pyroclastic rocks, which exceed 15 m in thickness, consist of laminated and massive crystal lithic lapilli tuff.

The tuffs are composed of up to 10–20 % juvenile lamproite lapilli with accidental rock fragments and angular grains of phlogopite, sanidine, plagioclase, richterite and quartz xenocrysts set in very finely comminuted lamproite ash. The angular rock fragments (2–5 mm in size) and quartz crystals are derived from disaggregated country rocks such as quartzite, siltstone, sandstone and volcanic lithics. Most of the lapilli grains show different degrees of alteration.

The lava flow ranges in thickness from 2 to 20 m and covers an area of about 0.03 km^2. Medium- to coarse-grained and flow-banded coherent lavas are located in the lava breccias. The top of the lava breccia has a

https://doi.org/10.1017/S0016756808004536 Published online by Cambridge University Press

vesicular texture with the vesicles elongated parallel to flow direction.

2.c. Bahçegüney lamproite

The dyke-like intrusion with the limited lava flow of lamproite is about 1 km long and 60 m in width and oriented approximately N–S. Lamproite intrudes the sedimentary formations of the Tauride Belt, including pebblestone, sandstone and siltstone alternations and latitic volcanic breccia. The lava flows are underlain by latitic volcanic breccia and overlain by thin pyroclastic deposits and lava breccia of the second phase latitic volcanic activity.

The massive and medium- to fine-grained lavas display well-developed thick lamination flow and elongated vesicles (reaching up to 4 cm). Along the contact of the massive lava flow, a baked zone approximately 50 cm thick is recognized by its red colour on the latitic volcanic breccia. Relatively fresh and coarse-grained massive lavas are observed in a deeply eroded small creek. Coarse sanidine phenocrysts reach up to 0.7 cm in size.

2.d. Göktepe lamproite

Subaerial lamproitic lava flows mainly cover sedimentary rocks of the Tauride belt and partly overlie the tephriphonolitic lava flow. Latitic pyroclastics, leucitite block and clast-rich volcaniclastic deposits and lacustrine sedimentary rocks mainly overlie lamproitic lavas. Flow types are variable, massive and vesicular with flow lamination, flow breccias and fine-grained coherent lava flows commonly present.

Flow alignment of platy phlogopite phenocrysts (up to 4 mm long) is a characteristic feature of massive and vesicular lavas. A wide range of vesicle morphologies is exhibited in the lavas and clasts. Red oxidized flow tops are observed at the top of the grey–light brownish grey lavas. Lava flows generally present medium- to fine-grained holocrystalline textures. The phenocrysts are elongated phlogopite and altered olivines.

3. Analytical methods

Quantitative analyses of mineral compositions were obtained at the Universite Pierre et Marie Curie (Laboratoire de Petrologie-Mineralogique), Paris, using an MS-46 CAMECA electron microprobe and CAMEBAX automated electron microprobe. Natural and synthetic minerals were used as standards. Counting time was 30 s; accelerating voltage was 15 kV; beam current was 20–30 nA; beam diameter was 5 μm. Whole-rock major, trace and rare earth element analyses were conducted by ICP-Emission Spectrometry (Jarrel Ash AtomComp Model 975/Spectro Ciros Vision) and ICP-Mass Spectrometry (Perkin-Elmer Elan 6000 or 9000) at ACME Analytical Laboratories, Vancouver, British Columbia (Canada).

Whole-rock Sr and Nd isotopic compositions were determined at the Institute of Geology and Geophysics, Chinese Academy of Sciences/Beijing, China. For Nd–Sr isotope analyses, Rb–Sr and light rare-earth elements were isolated on quartz columns by conventional ion exchange chromatography with a 5 ml resin bed of AG 50W-X12 (200–400 mesh). Nd and Sm were separated from other rare-earth elements on quartz columns using 1.7 ml of Teflon powder coated with HDEHP, di (2-ethylhexyl)-orthophosphoric acid, as the cation exchange medium. Sr was loaded with a Ta-HF activator on pre-conditioned W filaments and was measured in single-filament mode. Nd was loaded as phosphate on pre-conditioned Re filaments and measurements were performed in a Re double filament configuration. The $^{87}Sr/^{86}Sr$ and $^{143}Nd/^{144}Nd$ ratios are normalized to $^{86}Sr/^{88}Sr = 0.1194$ and $^{146}Nd/^{144}Nd = 0.7219$, respectively. In the Laboratory for Radiogenic Isotope Geochemistry of the IGG CAS, repeated measurements of Ames metal and the NBS987 Sr standard in year 2004/2005 gave mean values of 0.512149 ± 0.000003 ($n = 98$) for the $^{143}Nd/^{144}Nd$ ratio and 0.710244 ± 0.000004 ($n = 100$) for the $^{87}Sr/^{86}Sr$ ratio. The external precision is a 2σ uncertainty based on replicate measurements on these standard solutions over one year. Total procedural blanks were < 300 pg for Sr and < 50 pg for Nd.

4. Mineralogy

As seen in Figure 3, the lava flows and medium- to coarse-grained dyke and dome-shaped lamproite samples display fine-grained to coarse-grained holocrystalline textures, respectively. Their mineralogical compositions consist of sanidine, olivine, phlogopite, K-richterite, clinopyroxene, apatite, calcite and opaque minerals. They have phenocrysts of olivine, phlogopite, clinopyroxene and K-richterite.

Poikilitic and equant sanidine crystals constitute about 60 vol. % of the rock, and are found as clear and unaltered groundmass crystals (Fig. 3). Twinning is typically absent, but rare Carlsbad-twins have been noted. Generally, the crystal sizes range from 500 μm to 2 mm, but in the İlyasli lamproite they exceed 1 cm. In the fine-grained lamproite samples, sanidine crystals are less than 500 μm in size. Usually they contain inclusions of euhedral/subhedral phlogopite, clinopyroxene, apatite and opaque. Euhedral crystals are observed in the vugs, which coexist with calcite (Fig. 4a). Sanidines ($Or_{83–90}$) contain a relatively high abundance of Na_2O (1.11–1.69 wt %) and total FeO (1.35–1.61 wt %) and less than 0.03 wt % CaO. The concentrations of TiO_2 (0.11–0.28 wt %) and Al_2O_3 (17 wt %) are comparable to those of typical sanidines from lamproites worldwide (Mitchell & Bergman, 1991) (Table 1).

https://doi.org/10.1017/S0016756808004536 Published online by Cambridge University Press

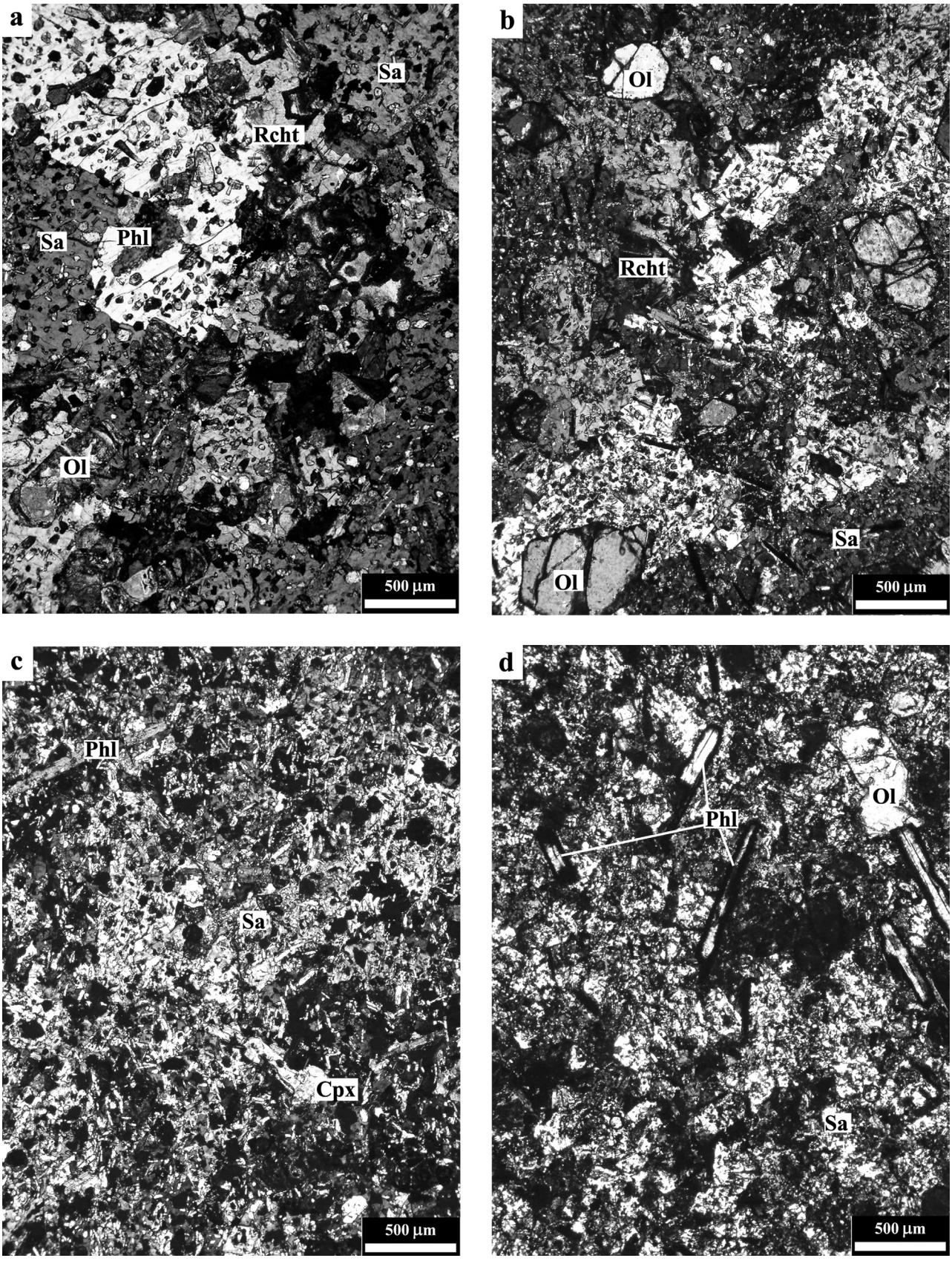

Figure 3. Photomicrographs of the massive lamproite lavas from İlyaslı lamproite (a), Mursalini lamproite (b), Bahçegüney lamproite (c), and lava flows of Göktepe lamproite outcrops (d).

https://doi.org/10.1017/S0016756808004536 Published online by Cambridge University Press

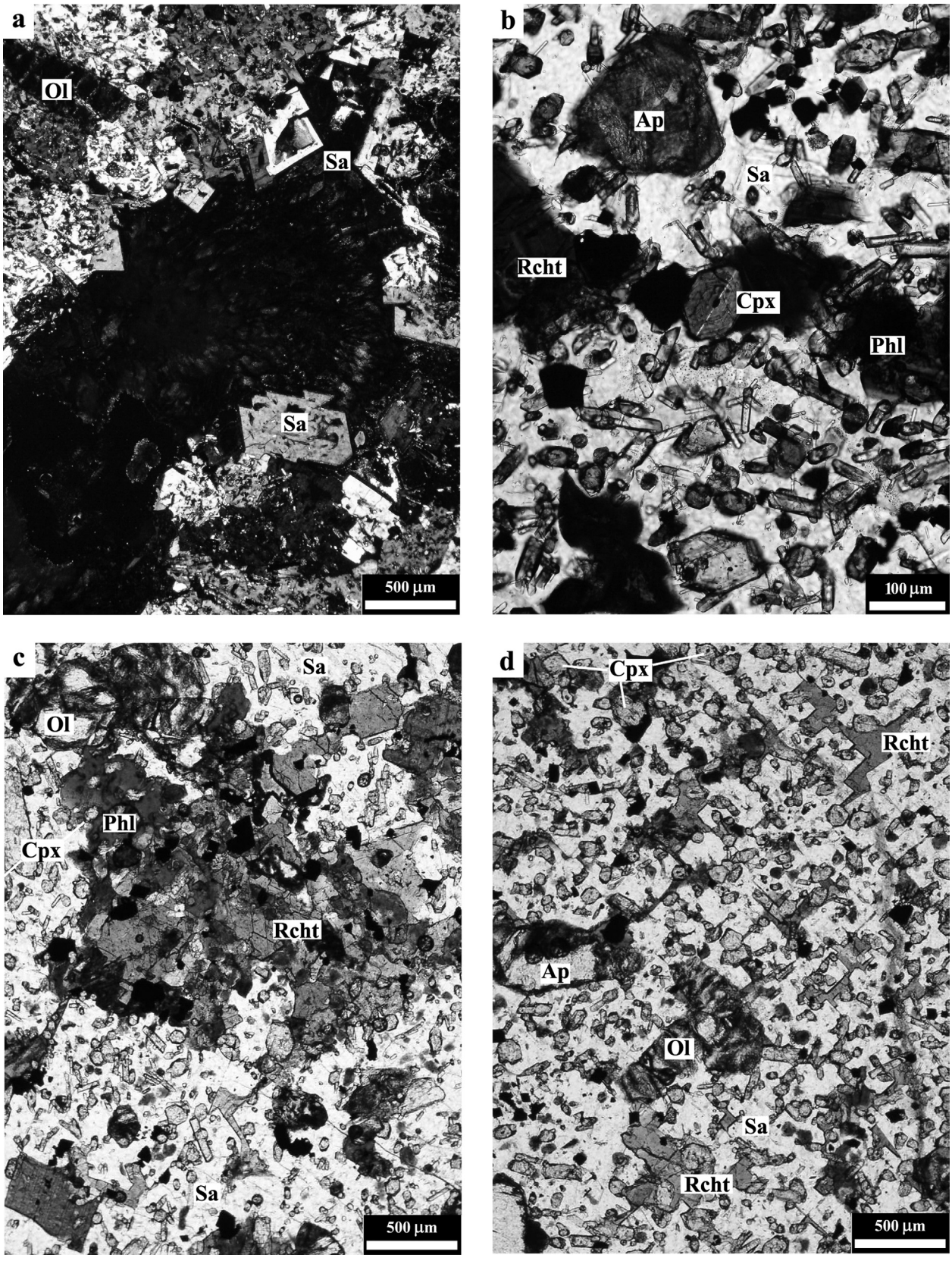

Figure 4. (a) Euhedral sanidine crystals in vugs. (b) Optically zoned euhedral clinopyroxene microcrysts showing simple twinning in cross-polars and plane polarized light. Anhedral richterite microphenocrysts and phenocrysts are easily distinguished by their reverse pleochroism colours. (c) Optically continuous poikilitic allotriomorphic richterite plates and euhedal richterite. (d) Interstitial anhedral richterite. Mineral symbols have been given according to Kretz (1983).

https://doi.org/10.1017/S0016756808004536 Published online by Cambridge University Press

Table 1. Representative mineral analyses of Afyon lamproites

	Sanidine					Phlogopite					Amphibole					
Analysis no.	2	3	21	41	69	1–4	3–15	4–16	5–31	8–64	25	26	27	35	38	42
SiO_2	64.63	64.04	64.42	64.89	64.17	39.64	37.63	37.53	37.68	37.68	53.10	53.02	52.52	51.87	53.29	51.90
TiO_2	0.26	0.20	0.23	0.11	0.28	8.07	8.19	6.80	6.63	6.48	4.46	3.35	4.31	2.98	3.36	4.55
ZrO_2											0.16	0.03	0.11	0.33	0.07	0.12
Al_2O_3	17.66	17.74	17.75	17.38	17.84	10.05	11.48	11.57	11.64	11.51	1.51	1.29	1.38	3.80	1.14	1.59
FeO*	1.35	1.41	1.44	1.54	1.61	11.13	9.91	9.21	9.10	9.12	7.95	6.91	7.90	7.66	6.81	8.01
MnO	bld	bld	bld	0.05	bld	0.22	0.10	0.09	0.18	0.08	0.15	0.13	0.10	0.14	0.14	0.17
MgO	bld	bld	bld	bld	bld	17.34	17.25	18.02	18.20	18.50	17.56	18.20	17.31	15.07	18.37	17.03
CaO	0.03	bld	bld	bld	bld	bld	bld	bld	bld	bld	5.67	6.03	5.52	5.63	5.96	6.06
SrO	0.04	0.07	0.08	bld	0.07	0.03	0.03	0.08	0.06	0.05	0.09	0.09	0.08	0.12	0.08	0.07
BaO	0.22	0.64	0.33	0.09	0.56	bld	1.99	2.65	1.93	2.23						
Na_2O	1.11	1.69	1.65	1.59	1.69	0.40	0.41	0.38	0.36	0.38	5.61	5.33	5.48	5.59	5.18	5.30
K_2O	14.94	13.75	13.80	13.93	13.00	9.89	8.57	8.55	8.54	8.21	2.56	2.79	2.63	3.92	2.71	2.57
F						1.24	1.24	1.24	1.24	1.24						
Total	100.3	99.6	99.7	99.6	99.3	98.0	96.8	96.2	95.6	95.5	98.8	97.2	97.4	97.2	97.1	97.4
Si	2.99	2.98	2.99	3.01	3.00	5.75	5.58	5.58	5.60	5.61	7.62	7.68	7.64	7.56	7.73	7.58
Ti	0.01	0.01	0.01	0.01	0.01	0.88	0.91	0.76	0.74	0.73	0.48	0.36	0.47	0.33	0.37	0.50
Zr											0.01	0.00	0.01	0.02	0.00	0.01
Al	0.96	0.97	0.97	0.95	0.98	1.72	2.01	2.03	2.04	2.02	0.26	0.22	0.24	0.65	0.20	0.27
Fe	0.05	0.05	0.06	0.06	0.06	1.35	1.23	1.14	1.13	1.14	0.95	0.84	0.96	0.93	0.83	0.98
Mn						0.03	0.01	0.01	0.02	0.01	0.02	0.02	0.01	0.02	0.02	0.02
Mg						3.75	3.81	3.99	4.03	4.11	3.76	3.93	3.76	3.27	3.97	3.71
Ca											0.87	0.93	0.86	0.88	0.93	0.95
Sr						0.00	0.00	0.01	0.00	0.00	0.01	0.01	0.01	0.01	0.01	0.01
Ba	0.00	0.01	0.01	0.00	0.01	0.00	0.12	0.15	0.11	0.13						
Na	0.10	0.15	0.15	0.14	0.15	0.11	0.12	0.11	0.10	0.11	1.56	1.50	1.55	1.58	1.46	1.50
K	0.88	0.82	0.82	0.83	0.78	1.83	1.62	1.62	1.62	1.56	0.47	0.52	0.49	0.73	0.50	0.48
An	–	–	–	–	–											
Ab	10	16	15	15	16											
Or	90	84	85	85	83											
Ann						0.26	0.24	0.22	0.22	0.22						
Phl						0.74	0.76	0.78	0.78	0.78						

Table 1. Continued.

	Clinopyroxene								Olivine								
	Core	>	Rim	Core	Rim	Core	>	Rim									
Analysis no.	3–18	3–19	3–20	5–39	4–40	5–45	5–47	5–48	23	24	59	68	70	184	185	5	3
SiO_2	53.09	53.46	52.15	53.68	54.02	53.44	53.39	52.69	38.35	38.47	38.91	38.00	38.29	38.63	38.43	39.20	38.67
TiO_2	0.50	0.53	0.81	0.31	0.39	0.46	0.50	0.76	bld	bld	bld	bld	bld	0.04	0.02	0.02	0.09
ZrO_2	bld	bld	bld	bld	bld	bld	bld	bld									
Al_2O_3	0.60	0.52	0.76	0.37	0.41	0.66	0.59	0.71	bld	bld	bld	bld	bld	bld	bld	bld	bld
Cr_2O_3									bld	bld	bld	bld	bld	bld	bld	0.06	bld
FeO*	4.55	3.92	5.77	4.39	4.15	4.61	4.45	5.72	21.62	21.08	18.49	20.42	20.11	20.03	21.24	17.92	20.41
MnO	0.14	0.10	0.24	0.16	0.11	0.12	0.10	0.19	0.48	0.44	0.38	0.47	0.44	0.41	0.54	0.64	0.75
NiO	0.07	bld	bld	0.02	bld	bld	bld	bld	bld	bld	bld	bld	bld	bld	bld	0.12	bld
MgO	17.28	17.42	16.07	17.83	17.66	17.33	17.13	16.44	40.08	40.67	42.82	40.53	41.75	40.56	38.94	41.94	40.66
CaO	23.30	23.06	22.08	22.60	22.58	22.16	22.47	21.74	0.22	0.23	0.20	0.22	0.16	0.16	0.14	0.25	0.23
Na_2O	0.22	0.19	0.52	0.16	0.14	0.23	0.32	0.49	bld	bld	0.03	bld	0.02	bld	bld	0.05	0.05
K_2O	bld	bld	0.04	bld	0.04	0.06	bld	0.02	bld	bld	bld	bld	bld	bld	bld	bld	bld
Total	99.8	99.2	98.5	99.6	99.5	99.1	99.0	98.8	100.8	100.9	100.8	99.7	100.8	99.8	99.3	100.2	100.8
Si	1.94	1.96	1.94	1.96	1.98	1.97	1.97	1.95	0.98	0.98	0.98	0.98	0.97	1.00	1.00	1.00	0.99
Ti	0.01	0.01	0.02	0.01	0.01	0.01	0.01	0.02									
Al	0.03	0.02	0.03	0.02	0.02	0.03	0.03	0.03									
Fe^{3+}	0.08	0.03	0.08	0.05	0.02	0.03	0.04	0.05	0.03	0.03	0.04	0.04	0.05	0.01	−0.01	0.00	0.02
Fe^{2+}	0.06	0.09	0.10	0.09	0.11	0.11	0.10	0.13	0.43	0.42	0.35	0.40	0.37	0.43	0.47	0.38	0.41
Mn	0.00	0.00	0.01	0.01	0.00	0.00	0.00	0.01	0.01	0.01	0.01	0.01	0.01	0.01	0.01	0.01	0.02
Mg	0.94	0.95	0.89	0.97	0.96	0.95	0.94	0.91	1.53	1.55	1.61	1.56	1.58	1.56	1.52	1.59	1.55
Ca	0.91	0.91	0.88	0.89	0.89	0.87	0.89	0.86	0.01	0.01	0.01	0.01	0.00	0.00	0.00	0.01	0.01
Na	0.02	0.01	0.04	0.01	0.01	0.02	0.02	0.04									
Fo									76.77	77.47	80.50	77.97	78.74	78.31	76.57	80.67	78.03
Fa									23.23	22.53	19.50	22.03	21.26	21.69	23.43	19.33	21.97
Mg number	87.13	88.79	83.23	87.86	88.35	87.02	87.28	83.67									
Wo	45.69	45.72	44.93	44.33	44.73	44.34	45.06	44.15									
En	47.14	48.06	45.52	48.69	48.68	48.26	47.81	46.48									
Fs	7.18	6.22	9.56	6.98	6.58	7.39	7.13	9.37									

FeO* – total iron as FeO; Fe^{2+} and Fe^{3+} have been recalculated after Morimoto (1989); bld – below detection limit. > is transition area from core to rim. An – albite; An – anorthite; Or – orthoclase; Ann – annite; Phl – phlogopite; Fo – forsterite; Fa – fayalite; Wo – wollastonite; En – enstatite; Fs – ferrosilite.

Strongly pleochroic phlogopite phenocrysts and microphenocrysts form lath-shaped and poikilitic plates containing euhedral apatite and stubby microcrystal pyroxene inclusions. Representative microprobe analyses of phlogopite phenocrysts are given in Table 1. The phlogopites in the İlyaslı lamproite contain high titanium (up to 8.1 wt % TiO_2), low alumina (up to 11.6 wt % Al_2O_3), barium (up to 2.2 wt %), and low total iron (up to 11 wt % total FeO) contents. In Figure 5, phlogopites follow the typical lamproite trend (Mitchell & Bergman, 1991).

Richterite-type amphiboles, distinguished by their distinctive pink to brownish-yellow pleochroism, are one of the typical minerals for lamproites (Fig. 4c, d). The richterite inclusions are unusual in the poikilitic sanidine crystals. Euhedral prisms (< 160 μm) are rare and generally observed as microcrysts at the contacts of sanidines or in the vugs of the lava. They crystallized contemporaneously with and/or after sanidine. In the coarse-grained part of İlyaslı lamproite, richterite crystals are found as optically continuous poikilitic allotriomorphic plates, euhedral phenocrysts (Fig. 4c) and interstitial anhedral grains (Fig. 4d). Richterites belong to the sodic–calcic amphibole group of Leake (1978), and their general formula is $(Na,K)NaCa(Mg,Fe^{2+})_5Si_8O_{22}(OH)_2$. Representative compositions of amphibole from İlyaslı lamproite (Table 1) show that they contain < 3 wt % TiO_2, 0.5–0.6 wt % Al_2O_3 and $Mg/(Mg+Fe_{tot})$ ratios of 0.8. The compositions of the amphibole are very close to the theoretical richterite composition of Wagner & Velde (1986).

Subhedral to euhedral olivine phenocrysts and microphenocrysts (reaching up to 2.5 mm in size) in various proportions are common constituents of lamproites (Fig. 3a, b, d). They do not show any kink bands and are interpreted to be of purely magmatic and not of xenocrystic origin. Olivine compositions range in Mg number from 76.6 to 80.7. They are magnesium- and manganese-poor (38–41 wt % MgO; 0.38–0.75 wt % MnO) relative to other Mediterranean lamproites. Calcium is usually low (< 0.25 wt % CaO), as are chromium (< 0.06 wt % Cr_2O_3) and nickel (< 0.12 wt % NiO) (Table 1). Olivine phenocrysts from Mediterranean lamproites are plotted in Figure 6 to compare with Afyon lamproites (dataset for Mediterranean lamproites is from Prelević & Foley, 2007). Olivine phenocrysts from Afyon lamproites have low CaO and Fo contents in respect to olivine phenocrysts of Mediterranean lamproites.

Clinopyroxene is generally present as slender or stubby lath-shaped microphenocrysts and groundmass microcrysts (100 μm to 200 μm in size). Microphenocrysts, reaching up to 750 μm in size, have subhedral stubby and partly rounded crystal forms. They are colourless to very pale green and weakly pleochroic. They occur as single and optically zoned crystals (Fig. 4b). Twinning is rare, but when present, it occurs

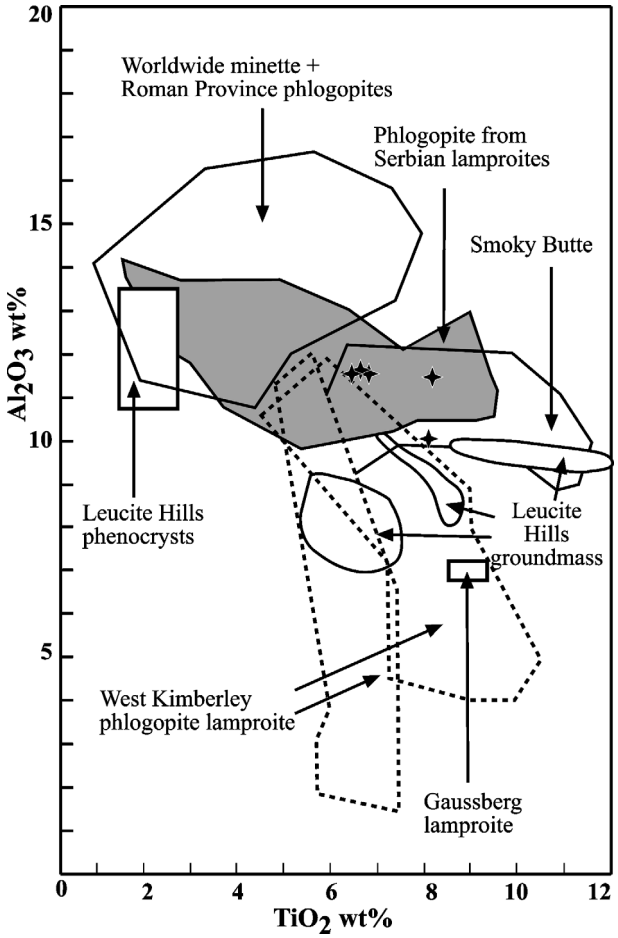

Figure 5. TiO_2 v. Al_2O_3 (wt %) diagram for phlogopite from Afyon lamproites. Data fields from Mitchell & Bergman (1991). Field for Serbian lamproites is from Prelević *et al.* (2005). Field for Gaussberg lamproite is from Sheraton & Cundari (1980).

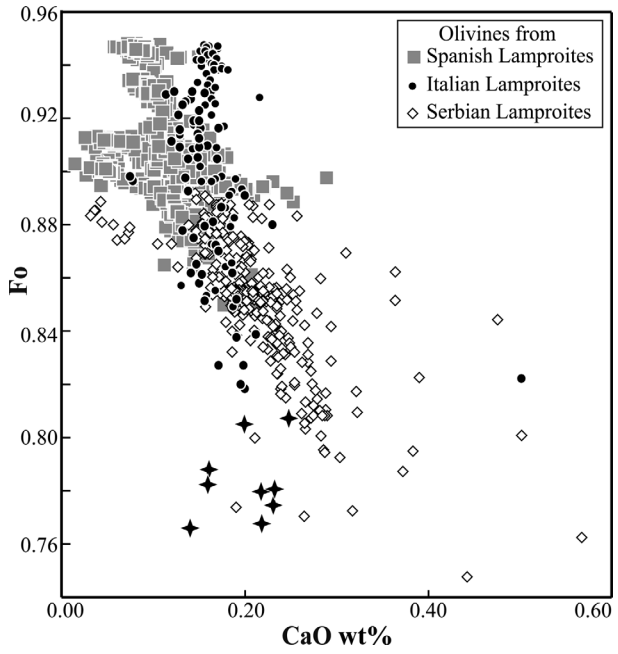

Figure 6. Plot of Fo v. CaO for olivines from samples of Afyon lamproites (black stars). Comparison dataset for primitive Mediterranean lamproites is from Prelević & Foley (2007).

https://doi.org/10.1017/S0016756808004536 Published online by Cambridge University Press

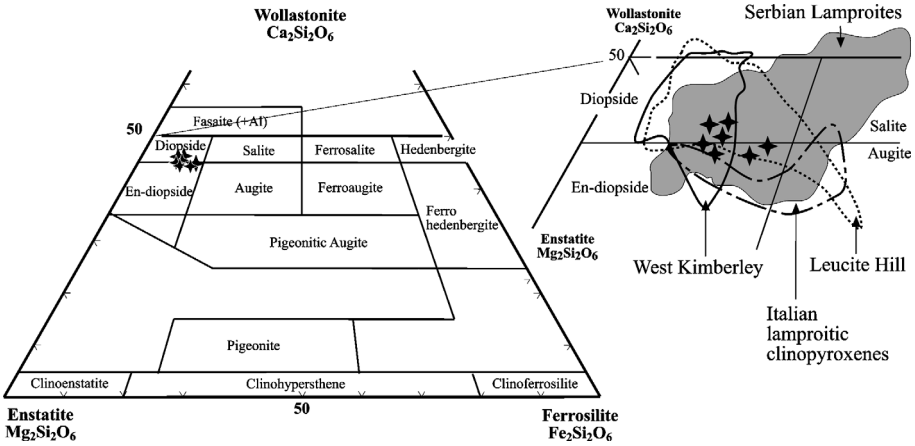

Figure 7. Clinopyroxene compositions of the İlyaslı lamproite plotted in the conventional Ca–Mg–Fe+Mn quadrilateral diagram. Data fields for Leucite Hill, West Kimberley and Italian lamproitic clinopyroxenes are from Mitchell & Bergman (1991) and Carlier & Lorand (2003), respectively.

as a simple twin with a composition plane parallel to (010). Microphenocrysts have Mg number 83–87 and very low amounts of Ti and Al (Table 1) This is a peculiar feature of clinopyroxene from lamproitic rocks (Mitchell, 1985). They are diopside–En-diopside ($En_{47–49}Fs_{7–9}Wo_{44–46}$) similar to clinopyroxenes from West Kimberley, Leucite Hill and Serbian lamproites (e.g. Mitchell & Bergman, 1991; Carlier & Lorand, 2003; Prelević *et al.* 2005) (Fig. 7).

Apatites are mainly colourless euhedral acicular hexagonal prisms (up to 80 μm × 200 μm) and include minute fluid inclusions. The groundmass apatite crystals reach up to 40 μm × 100 μm in diameter. Subhedral/anhedral apatite xenocrysts are rich in fluid inclusions. Carbonate and barite crystals occur as vug fillings in the medium–coarse-grained lamproites.

5. Bulk-rock geochemistry

The bulk-rock major and trace element compositions of representative coarse-grained lamproite samples are given in Table 2. Their major element contents have relatively high SiO_2(50–51 wt %), low Al_2O_3 (9–10 wt %), MgO > 3 %, K_2O > 3 %, K_2O/Na_2O > 3, and mostly plot in Group I (lamproite field) and Group III (Roman type) in the ultrapotassic rock classification diagram (Al_2O_3 v. CaO) of Foley *et al.* (1987) and Foley (1992*a*, 1994) (Fig. 8a). In the CaO/SiO_2 and CaO/MgO diagrams (Fig. 8b, c) they plot partly in the Roman province field, and overlap the potassium series, transitional rock and high-potassium series rocks of the Italian province (e.g. Conticelli & Peccerillo, 1992; Peccerillo, 1995, 2003; Conticelli *et al.* 2002). Mg number ranges from 49.3 to 72.7, and they show low Ni contents, below 258 ppm. TiO_2 contents of the samples are < 1.5 wt %, which is a characteristic of orogenic alkaline rocks, as proposed by Thompson (1997) and Rogers (1992). Based on P_2O_5/TiO_2 v. TiO_2 ratios to describe the geological setting of ultrapotassic rocks (Foley *et al.* 1987), Afyon lamproites reflect an active orogenic area with low TiO_2 contents (1–2 wt %) relative to the stable continental area (Fig. 8d). The incompatible trace elements show extreme enrichment in large ion lithophile elements (LILE; Cs, Rb, Ba, Th and U), 200 to 8000 times primitive mantle of Sun & McDonough (1989). Samples display high abundances of Cs, Rb, Ba, Th, Pb and Sr. Primitive mantle-normalized element patterns of Afyon lamproites show characteristic Pb and K peaks, but they do not exhibit Ba, Sr and P troughs, as are observed in all the other Mediterranean lamproites (Fig. 9). Afyon lamproites are depleted in high field strength elements (HFSE) but show positive Sr and negative Nd anomalies with respect to those of the lamproitic rocks of Spain, Italy and Serbia. Afyon samples also display high LILE/HFSE and LILE/REE values, characteristic of magmas related to an orogenic environment (Conticelli *et al.* 2002). Chondrite-normalized (Sun & McDonough, 1989) rare earth element (REE) patterns (Fig. 10) of Mediterranean lamproites display a pronounced enrichment of LREE over HREE with $(La/Yb)_{cn}$ values ranging from 15.2 to 17.0 and negative Eu anomalies ($Eu/Eu^* = 0.73–0.77$). Afyon lamproites show similarities with REE patterns and Eu anomalies; however, they are less fractionated than Italian, Spanish and Serbian lamproites ($(La/Yb)_{cn} = 21–112$).

5.a. Nd–Sr isotopes

The Nd and Sr isotopic ratios of Afyon lamproites are reported in Table 2. They yield a range of high initial $^{87}Sr/^{86}Sr$ ratios (0.707703–0.708073) and low $^{143}Nd/^{144}Nd$ ratios (0.512380–0.512438). The samples plot in the enriched quadrant below bulk earth values and approach upper continental crustal values, which are typical for ultrapotassic rocks derived from either an enriched mantle or a mantle source contaminated by crustal material (Mitchell & Bergman, 1991). Afyon lamproites show similarity to other lamproitic rocks in

https://doi.org/10.1017/S0016756808004536 Published online by Cambridge University Press

Table 2. Major (%) and trace element (ppm) and Sr and Nd isotopes of Afyon lamproite samples

Sample no.	IL 90	IL 106	MR 107/4	MR 107/5	BH 114/2	BH 114/5
SiO_2	50.65	51.41	52.42	52.4	50.84	50.46
TiO_2	1.36	1.35	1.37	1.36	1.07	1.07
Al_2O_3	10.03	10.22	9.99	10.01	9.38	9.32
Fe_2O_3	7.07	6.9	9.62	9.69	6.6	6.45
MnO	0.13	0.18	0.36	0.41	0.12	0.19
MgO	6.35	5.09	4.56	4.29	8.01	7.02
CaO	8.36	8.54	5.94	5.61	8.18	9.20
Na_2O	1.31	1.55	1.43	1.43	1.34	1.42
K_2O	7.81	7.87	6.52	6.97	7.49	7.31
P_2O_5	1.56	1.62	1.68	1.62	1.41	1.48
Cr_2O_3	0.02	0.02	0.02	0.02	0.08	0.08
LOI	4.70	4.60	5.40	5.50	4.80	5.30
Total	99.35	99.35	99.31	99.31	99.32	99.30
Mg number	71.7	62.2	51.4	49.7	72.7	70.8
K_2O/Na_2O	3.92	3.34	3.00	3.21	3.68	3.39
K_2O/Al_2O_3	0.84	0.83	0.71	0.75	0.86	0.85
Ba	3437	3516	3784	3773	3428	3468
Cu	74	86	39	55	62	64
Nb	26.9	26	27.9	29	22.4	21.1
Ta	1.6	1.5	1.7	1.8	1.3	1.3
Ni	48	40	64	58	258	211
Pb	33	30	32	32	31	32
Rb	194.6	266.6	383.0	419.2	213.2	538.8
Sr	1168.7	1140.7	1106.8	1083.1	1226.2	1230.1
V	141	141	141	142	101	104
Zr	440.5	427.9	455.9	469.5	360.8	353.3
Zn	72	71	84	82	64	66
Y	25.8	25.6	26.4	26.1	23.7	22.9
Th	19.9	18.5	18.9	19.4	14.2	13.3
U	6.6	6.0	4.3	4.3	4.0	4.9
Ce	94.7	94.3	98.9	96.9	83.2	81
La	45.2	45.3	47.7	48.1	43.5	41.8
Cs	2.0	18.4	55.4	40.6	3.1	46.1
Sm	10.1	9.7	9.8	10.1	8.4	7.9
Nd	47.8	47.1	47.8	46.1	36.8	35.7
Er	2.51	2.61	2.73	2.55	2.3	2.17
Eu	2.04	2.14	2.18	2.09	1.59	1.67
Ga	15.5	14.8	15.2	15.9	13.6	12.8
Gd	7.30	7.43	7.7	7.32	6.35	6.01
Hf	11.9	11.3	12.6	12.7	9.4	9.4
Ho	0.83	0.81	0.85	0.85	0.76	0.69
Dy	5.2	5.36	5.46	5.28	4.54	4.61
Lu	0.3	0.29	0.31	0.29	0.27	0.25
Pr	11.70	11.63	11.65	11.57	9.35	9.25
Tb	0.96	0.95	0.97	0.99	0.84	0.79
Tm	0.32	0.33	0.30	0.30	0.27	0.27
Yb	2.04	2.13	2.12	2.03	1.86	1.81
$(La/Yb)_{CN}$	15.89	15.26	16.14	17.00	16.78	16.57
$(Tb/Yb)_{CN}$	2.13	2.02	2.07	2.20	2.04	1.97
Eu/Eu^*	0.73	0.77	0.77	0.74	0.67	0.74
$^{87}Sr/^{86}Sr)_m$	0.70800	0.70794	0.70783	0.70878	0.70814	0.70812
$^{87}Sr/^{86}Sr)_i$	0.70793	0.70784	0.70770	0.70771	0.70808	0.70794
$^{143}Nd/^{144}Nd)_m$	0.51239	0.51245	0.51244	0.51242	0.51240	0.51244
$^{143}Nd/^{144}Nd)_i$	0.51238	0.51244	0.51243	0.51241	0.51239	0.51243

IL – İlyaslı Lamproite; MR – Mursalini Lamproite; BH – Bahçegüney Lamproite. Total iron as Fe_2O_3. Mg number = atomic $100Mg/(Mg+0.9Fe_T)$; 2 sigma for isotopic analyses is between 0.000001 and 0.000005 for Nd isotopic measurements, and between 0.000001 and 0.000005 for Sr isotopic measurements.

Eastern Mediterranean ultrapotassic provinces. Their isotopic compositions overlap with lamproites from Macedonia and Serbia and have higher Nd and lower Sr isotopic ratios than Italian and Spanish lamproites and Roman Province ultrapotassic rocks (Fig. 11).

6. Discussion and conclusions

Lamproites within the Mediterranean region are part of the Alpine–Himalayan orogenic belt. They are common in the Mediterranean and are located in four regions: Italy (e.g. Venturelli *et al.* 1984*b*; Peccerillo, Poli & Serri, 1988; Conticelli *et al.* 2007), Spain (e.g. Venturelli *et al.* 1984a; Benito *et al.* 1999; Duggen *et al.* 2005), Serbia and Macedonia (Prelević *et al.* 2005; Altherr *et al.* 2004) and Turkey (e.g. Savaşçın & Oyman, 1998; Francalanci *et al.* 2000; Çoban & Flower, 2006).

Lamproitic rocks of the Mediterranean region are mainly related to subduction and collisional orogenic

https://doi.org/10.1017/S0016756808004536 Published online by Cambridge University Press

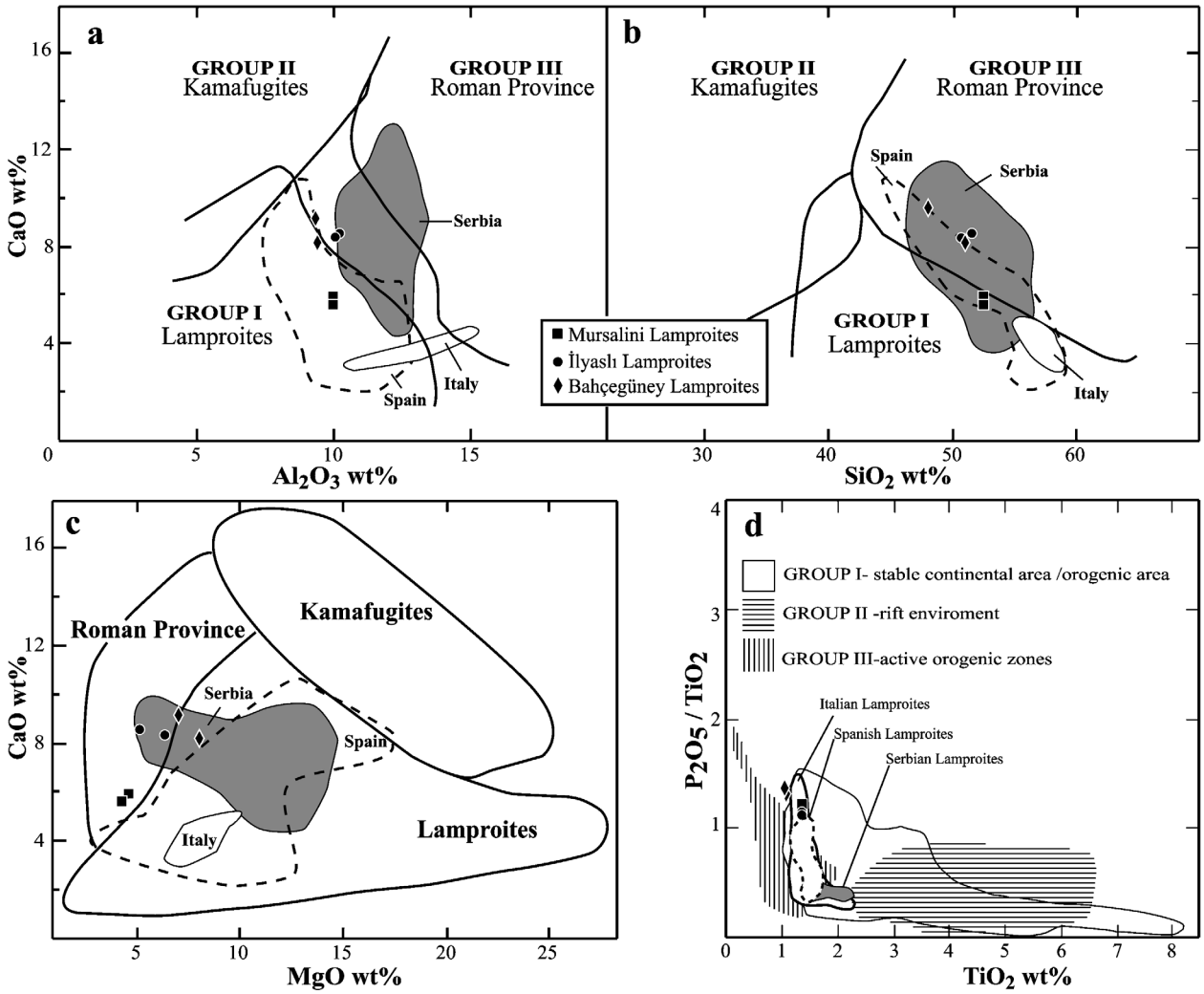

Figure 8. Plots of Afyon lamproites on ultrapotassic rock classification diagrams of Foley *et al.* (1987) and Foley (1992*a*, 1994). Field for Italian lamproites is from Peccerillo, Poli & Serri (1988); Conticelli (1998); Conticelli, Manetti & Menichetti (1992) and Conticelli *et al.* (2002). Fields for Spanish and Serbian lamproites are from Duggen *et al.* (2005) and Prelević *et al.* (2005), respectively.

processes and/or are followed by an extensional regime resulting after the convergence of Africa and Eurasia. During subduction processes, the depleted lithospheric mantle source was affected by subduction-derived metasomatising agents (e.g. Nelson, McCulloch & Sun, 1986; Ellam *et al.* 1989; Peccerillo, 1992). The occurrences of lamproitic melts are explained either by partial melting of previously depleted lithospheric mantle metasomatically enriched by fluids or melts from earlier subduction processes or source contamination by subducted continental crustal material (e.g. Peccerillo, 1985, 1999, 2003; Rogers *et al.* 1985; Beccaluva, Di Girolamo & Serri, 1991; Conticelli, 1998, Conticelli *et al.* 2002, 2004; Altherr *et al.* 2004; Duggen *et al.* 2005).

In the geodynamic history of the Aegean Sea and western Anatolia, the continental subduction–collision of the African Plate under the southern Eurasia Plate along the Hellenic and Cyprus arcs occurred during Middle–Late Miocene times (Fytikas *et al.* 1976; Doglioni *et al.* 2002; Agostini *et al.* 2007). This collisional phase was followed by an extensional tectonic regime which commenced during Late Miocene–Early Pliocene times in western Anatolia (Koçyiğit, 1984; Dewey & Şengör, 1979). Koçyiğit (1984) indicated that several NE–SW- and NW–SE-trending cross-graben and horst structures bounded by active normal faults dominate the area between Afyon and the Isparta Angle (Fig. 1). This period is also interpreted as the beginning of intra-plate rifting. Francalanci *et al.* (2000) argued that the alkaline magmatism was associated with an extensional tectonic phase and occurred along a N–S-trending tectonic line between Afyon to Isparta (Antalya fault zone).

The Afyon lamproites as defined by Foley *et al.* (1987) display many characteristics that are consistent with contamination of their mantle source by a subducted component. This indicates a role for subduction-related processes and modification of the mantle source by metasomatism. Afyon lamproites have relatively low

https://doi.org/10.1017/S0016756808004536 Published online by Cambridge University Press

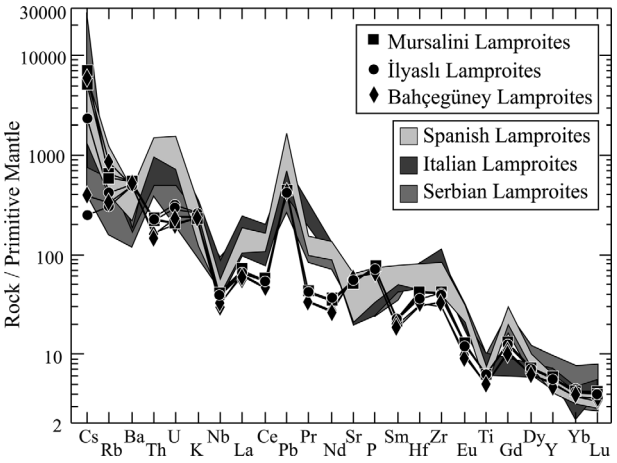

Figure 9. Primitive-mantle normalized incompatible element patterns of Afyon lamproites. Normalized values are after Sun & McDonough (1989). Field for Italian lamproites is from Peccerillo, Poli & Serri (1988); Conticelli (1998); Conticelli, Manetti & Menichetti (1992) and Conticelli *et al.* (2002). Fields for Spanish and Serbian lamproites are from Duggen *et al.* (2005) and Prelević *et al.* (2005), respectively.

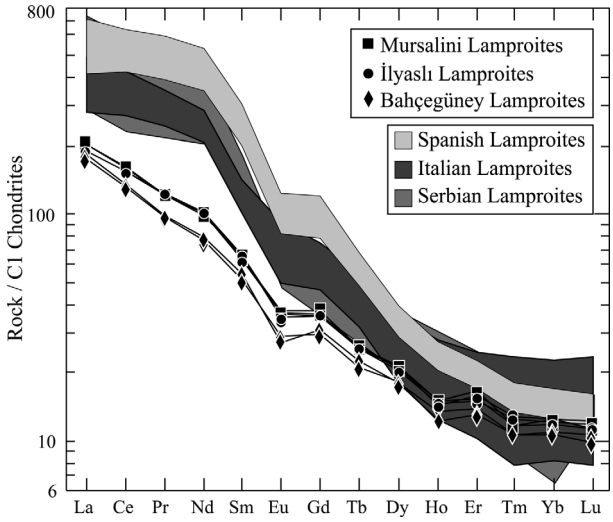

Figure 10. C1 Chondrite-normalized REE patterns of Afyon lamproites. Normalized values are after Sun & McDonough (1989). Field for Italian lamproites is from Conticelli (1998); Conticelli, Manetti & Menichetti (1992) and Conticelli *et al.* (2002). Fields for Spanish and Serbian lamproites are from Duggen *et al.* (2005) and Prelević *et al.* (2005), respectively.

Ti and Nb concentrations, and show strong enrichments of fluid-mobile elements (Rb, U, K, and Pb) relative to fluid-immobile, incompatible elements (Nb, Ta, Zr, Hf, REE) characteristic of magma generated in a subduction-related orogenic environment. This trace-element pattern indicates a crustal signature for Afyon lamproites. The negative Ti anomalies in the patterns suggest a Ti-rich accessory phase in their melting residues. Sr and Nd isotopic values plot in the enriched quadrant and overlap with lamproitic rocks from Serbia and Macedonia, suggesting a high amount of

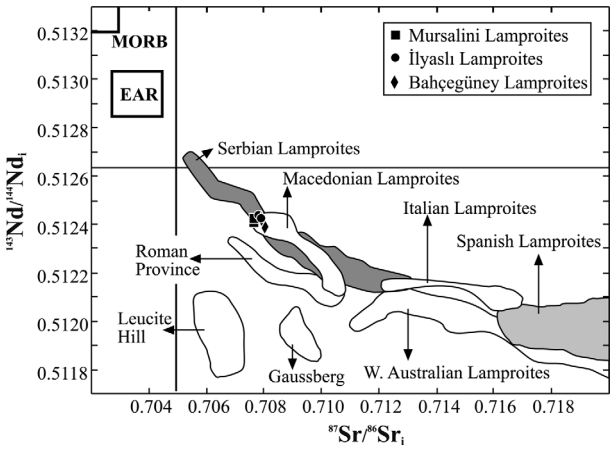

Figure 11. Nd–Sr isotope diagram (initial values) for Afyon lamproites. Also shown for comparison are fields for Serbian lamproites (Altherr *et al.* 2004; Prelević *et al.* 2005); Gaussberg (Murphy, Collerson & Kamber, 2002); Leucite Hills lamproites (Nelson, McCulloch & Sun, 1986); Italian lamproites and Roman Province (Conticelli *et al.* 2002); Spanish lamproites (Duggen *et al.* 2005); West Australian lamproites (Fraser *et al.* 1985); Macedonian lamproites (Altherr *et al.* 2004); MORB (Zindler & Hart, 1986); EAR – European asthenospheric reservoir (Cebria & Wilson, 1995).

contamination by crustal components from a subducted slab in their source.

Serbian lamproites defined by the recent study of Prelević, Foley & Cvetković (2007) are not contemporaneous with any subduction tectonics as Italian and Spanish lamproites are. According to these authors, the past subduction episodes have played a major role in conveyance of metasomatic inputs to the lithospheric mantle during collision. The alkaline melts of Serbian lamproites were produced by mantle mixing between the Serbian enriched mantle end-member (vein-material) and MORB-like end member (peridotite mantle) (Prelević, Foley & Cvetković, 2007) (Fig. 12). According to this model, which is consistent with vein + wall-rock melting (Foley, 1992*b*; Mitchell, 1995), Afyon lamproites indicate consistency with end-member mixing models of Serbian lamproites which are located on mixing curves of the crustal end-member Sr and Nd isotopic variations for Serbian lamproites. Hence, such a situation may be interpreted to generate alkaline melts by a crustal end-member mixing model for Afyon lamproites during the post-collisional tectonic regime in western Anatolia.

In general, Mediterranean lamproites have the same mineralogical composition consisting of olivine + clinopyroxene ± orthopyroxene + K-richterite + phlogopite + sanidine ± leucite + apatite ± dalyite ± Cr/Zr-armacolite + ilmenite + rutile + magnetite + hematite + spinel (e.g. Altherr *et al.* 2004; Conticelli *et al.* 2007; Prelević *et al.* 2005). The mineralogy of Afyon lamproites is characteristically similar to Mediterranean lamproites. Olivine is the main component of the Mediterranean lamproites.

https://doi.org/10.1017/S0016756808004536 Published online by Cambridge University Press

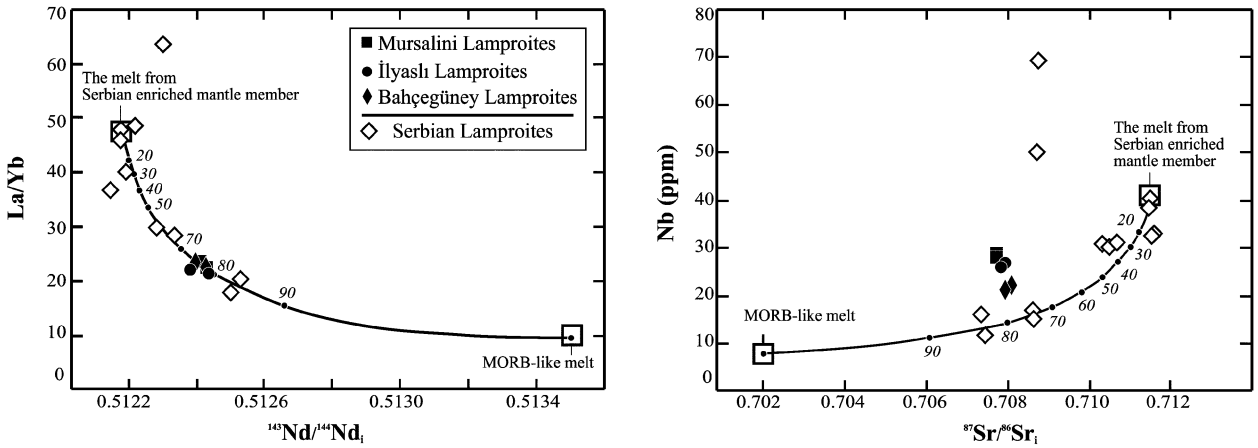

Figure 12. Placement of Afyon lamproites on the $^{143}Nd/^{144}Nd$ v. La/Yb and $^{87}Sr/^{86}Sr$ v. Nb (ppm) diagrams of primitive samples of Serbian lamproitic rocks showing possible end-members to explain the isotopic variation in their source (Prelević *et al.* 2005).

In olivines from Spanish and Italian lamproites, Fo contents are extremely high (82–94 % and 85–94 %, respectively). In Serbian lamproites, Fo content is widely variable (72–89 %). The olivine phenocrysts from Afyon lamproites have low Fo and CaO contents (76–81 % Fo). The very low calcium contents in olivine reflect the low level of CaO in the melt during magmatic differentiation or changes in melt composition during olivine crystallization (Libourel, 1999). Liquid experiments on Si-rich lamproites (e.g. Foley, 1992*a*; Mitchell & Edgar, 2002) show that olivine is notably absent as a liquidus phase at pressures in excess of 10 kbar. The presence of olivine has been reported only at low pressures, to somewhere between 2 and 3.0 Gpa, according to Edgar & Mitchell (1997), or 1.0 GPa according to Foley (1990). Foley (1992*a*) suggested that primary lamproitic magmas from leucite lamproite to olivine lamproite can be derived by partial melting of phlogopite harzburgite as a function of pressure between < 15 and 60 kbar. Prelević, Foley & Cvetković (2007) explain that the extraction depth of Mediterranean lamproites from the mantle source is less than 60 km.

In conclusion, Afyon lamproites display many features of Mediterranean-type lamproites at post-collision–extension areas related to subduction processes controlled by low-pressure fractionation. Afyon lamproites require crustal and mantle components and modification by metasomatism for their origin. Mantle mixing between an enriched mantle end-member (vein-material) and MORB-like end member (peridotite mantle) seems the most likely model for the alkaline melt of Afyon lamproites during extension processes.

Acknowledgements. I wish to thank Dr Dejan Prelević for his stimulating discussions and suggestions. I thank Hilary Downes and Sandro Conticelli for constructive reviews that significantly improved the paper. Editorial handling by David Pyle was very helpful. Special thanks are due to Philippe D'Arco for microprobe analyses carried out in the Université Pierre et Marie Curie (Laboratoire de Petrologie-Mineralogique), Paris. Thanks also to Hubert Remy for organizing and providing the electron-microprobe analyses.

References

AGOSTINI, S., DOGLIONI, C., INNOCENTI, F., MANETTI, P., TONARINI, S. & SAVAŞÇIN, M. Y. 2007. The transition from subduction-related to intraplate Neogene magmatism in the Western Anatolia and Aegean area. In *Cenozoic Volcanism in the Mediterranean Area* (eds L. Beccaluva, G. Banchini & M. Wilson), pp. 1–15. Geological Society of America, Special Paper no. 418.

AKAL, C. 2003. Mineralogy and geochemistry of melilite leucitites, Balçıkhisar, Afyon, Turkey. *Turkish Journal of Earth Sciences* **12**, 215–39.

ALICI, P., TEMEL, A., GOURGAUD, A., KIEFFER, G. & GÜNDOĞDU, M. N. 1998. Petrology and geochemistry of potassic rocks in the Gölcük area (Isparta, SW Turkey): genesis of enriched alkaline magmas. *Journal of Volcanology and Geothermal Research* **85**, 423–46.

ALTHERR, R., MEYER, H.-P., HOLL, A., VOLKER, F., ALIBERT, C., MCCULLOCH, M. T. & MAJER, V. 2004. Geochemical and Sr–Nd–Pb isotopic characteristics of Late Cenozoic leucite lamproites from the East European Alpine belt (Macedonia and Yugoslavia). *Contributions to Mineralogy and Petrology* **147**, 58–73.

BECCALUVA, L., DI GIROLAMO, P. & SERRI, G. 1991. Petrogenesis and tectonic setting of the Roman volcanic province, Italy. *Lithos* **26**, 191–221.

BENITO, R., LOPEZ-RUIZ, J., CEBRIA, J. M., HERTOGEN, J., DOBLAS, M., OYARZUN, R. & DEMAIFFE, D. 1999. Sr and O isotope constraints on source and crustal contamination in the high-K calc-alkaline and shoshonitic Neogene volcanic rocks of SE Spain. *Lithos* **46**, 773–802.

BESANG, C., ECKHARDT, F.-J., HARRE, W., KREUZER, H. & MÜLLER, P. 1977. Radiometrische altersbestimmungen an neogenen eruptivgesteinen der Türkei. *Geologisches Jahrbuch Reihe* **B 25**, 3–36.

CARLIER, C. & LORAND, J. P. 2003. Petrogenesis of a zirconolite-bearing Mediterranean-type lamproite from the Peruvian Altiplano (Andean Cordillera). *Lithos* **69**, 15–35.

https://doi.org/10.1017/S0016756808004536 Published online by Cambridge University Press

CEBRIA, J.-M. & WILSON, M. 1995. Cenozoic mafic magmatism in Western/Central Europe: A common European asthenospheric reservoir? *Terra Abstract* **8**, 162.

CONTICELLI, S. 1998. The effect of crustal contamination on ultrapotassic magmas with lamproitic affinity: mineralogical, geochemical and isotope data from the Torre Alfina lavas and xenoliths, Central Italy. *Chemical Geology* **149**, 51–81.

CONTICELLI, S., D'ANTONIO, M., PINARELLI, L. & CIVETTA, L. 2002. Source contamination and mantle heterogeneity in the genesis of Italian potassic and ultrapotassic volcanic rocks: Sr–Nd–Pb isotope data from Roman Province and Southern Tuscany. *Mineralogy and Petrology* **74**, 189–222.

CONTICELLI, S., CARLOS, R. W., WIDOM, E. & SERRI, G. 2007. Chemical and isotopic composition (Os, Pb, Nd and Sr) of Neogene to Quaternary calc-alkalic, shoshonitic, and ultrapotassic mafic rocks from the Italian peninsula: Inferences on the nature of their mantle sources. In *Cenozoic Volcanism in the Mediterranean Area* (eds L. Beccaluva, G. Banchini & M. Wilson), pp. 171–202. Geological Society of America, Special Paper no. 418.

CONTICELLI, S., MELLUSO, L., PERINI, G., AVANZINELLI, R. & BOARI, E. 2004. Petrologic, geochemical and isotopic characteristics of potassic and ultrapotassic magmatism in central-southern Italy; inferences on its genesis and on the nature of mantle sources. *Periodico di Mineralogia* **73**, special issue 1, 135–64.

CONTICELLI, S., MANETTI, P. & MENICHETTI, S. 1992. Mineralogy, geochemistry and Sr-isotopes in orendites from South Tuscany, Italy; constraints on their genesis and evolution. *European Journal of Mineralogy* **4**, 1359–75.

CONTICELLI, S. & PECCERILLO, A. 1992. Petrology and geochemistry of potassic and ultrapotassic volcanism in central Italy: petrogenesis and inferences on the evolution of the mantle sources. *Lithos* **28**, 221–40.

ÇOBAN, H. & FLOWER, M. F. J. 2006. Mineral phase compositions in silica-undersaturated 'leucite' lamproites from the Bucak area, Isparta, SW Turkey. *Lithos* **89**, 275–99.

DEWEY, J. F. & ŞENGÖR, A. M. C. 1979. Aegean and surrounding regions: complex multiplate and continuum tectonics in convergent zone. *Geological Society of America Bulletin* **90**, 84–92.

DOGLIONI, C., AGOSTINI, S., CRESPI, M., INNOCENTI, F., MANETTI, P., RIGUZZI, F. & SAVAŞÇIN, Y. 2002. On the extension in Western Anatolia and the Aegean sea. In *Reconstruction of the Evolution of the Alpine–Himalayan Orogen* (eds G. Rosenbaum & G. S. Lister), pp. 169–84. *Journal of the Virtual Explorer* **8**.

DUGGEN, S., HOERNLE, K., VAN DEN BOGAARD, P. & GARBE-SCHONBERG, D. 2005. Post-Collisional Transition from Subduction- to Intraplate-type Magmatism in the Westernmost Mediterranean: Evidence for Continental-Edge Delamination of Subcontinental Lithosphere. *Journal of Petrology* **46**, 1155–1201.

EDGAR, A. D. & MITCHELL, R. H. 1997. Ultra high pressure–temperature melting experiments on an SiO_2-rich lamproite from Smoky Butte, Montana; derivation of siliceous lamproite magmas from enriched sources deep in the continental mantle. *Journal of Petrology* **38**, 457–77.

ELLAM, R., HAWKESWORTH, C., MENZIES, M. & ROGERS, N. 1989. The volcanism of southern Italy: Role of subduction and the relationship between potassic and sodic alkaline volcanism. *Journal of Geophysical Research* **94**, 4589–601.

FOLEY, S. F. 1990. Experimental constraints on phlogopite chemistry in lamproites: 2. Effect of pressure-temperature variations. *European Journal of Mineralogy* **2**, 327–41.

FOLEY, S. F. 1992*a*. Petrological characterization of the source components of potassic magmas: geochemical and experimental constraints. *Lithos* **28**, 187–204.

FOLEY, S. F. 1992*b*. Vein-plus-wall-rock melting mechanisms in the lithosphere and the origin of potassic magmas. *Lithos* **28**, 435–53.

FOLEY, S. F. 1994. Geochemische und experimentelle Untersuchungen zur Genese der kalireichen Magmatite. *Neues Jahrbuch für Mineralogie-Abhandlungen* **167**, 1–55.

FOLEY, S. F., VENTURELLI, G., GREEN, D. H. & TOSCANI, L. 1987. The ultrapotassic rocks: characteristics, classification and constraints for petrogenetic models. *Earth Science Reviews* **24**, 81–134.

FRANCALANCI, L., CIVETTA, L., INNOCENTI, F. & MANETTI, P. 1990. Tertiary–Quaternary alkaline magmatism of the Aegean–Western Anatolian area: a petrological study in the light of new geochemical and isotopic data. In *Proceedings of the International Earth Sciences Colloquium of the Aegean Region* (eds M. Y. Savaşçın & A. H. Eronat), pp. 385–96. DEU, Izmir, Turkey.

FRANCALANCI, L., INNOCENTI, F., MANETTI, P. & SAVAŞÇIN, M. Y. 2000. Neogene alkaline volcanism of the Afyon–Isparta area, Turkey: petrogenesis and geodynamic implications. *Mineralogy and Petrology* **70**, 285–312.

FRASER, K., HAWKESWORTH, C., ERLANK, A., MITCHELL, R. & SCOTT-SMITH, B. 1985. Sr, Nd and Pb isotope and minor element geochemistry of lamproites and kimberlites. *Earth and Planetary Science Letters* **76**, 57–70.

FYTIKAS, M., GIULIANI, O., INNOCENTI, F., MARINELLI, G. & MAZZUOLI, R. 1976. Geochronological data on recent magmatism of the Aegean Sea. *Tectonophysics* **21**, 29–34.

INNOCENTI, F., AGOSTINI, T. S., DI VINCENZO, G., DOGLIONI, C., MANETTI, P., SAVAŞÇIN, M. Y. & TONARINI, S. 2005. Neogene and Quaternary volcanism in Western Anatolia: Magma sources and geodynamic evolution. *Marine Geology* **221**, 397–421.

KELLER, J. 1983. Potassic lavas in the orogenic volcanism of the Mediterranean area. *Journal of Volcanology and Geothermal Research* **18**, 321–35.

KELLER, J. & VILLARI, L. 1972. Rhyolitic ignimbrites in the region of Afyon (central Anatolia). *Bulletin Volcanologique* **36**, 342–58.

KOÇYIĞIT, A. 1984. Intra-plate neotectonic development in southwestern Turkey and adjacent areas. *Bulletin Geological Society of Turkey* **27**, 1–15.

KRETZ, R. 1983. Symbols for rock-forming minerals. *American Mineralogist* **68**, 277–9.

LEAKE, B. E. 1978. Nomenclature of Amphiboles. *Mineralogical Magazine* **42**, 533–63.

LEFEVRE, C., BELLON, H. & POISSON, A. 1983. Presence de leucitites dans le volcanism Pliocene de la region d'Isparta (Taurides occidentales, Turquie). *Comptes Rendus de l'Academie des Sciences* **297**, 367–72.

LIBOUREL, G. 1999. Systematics of calcium partitioning between olivine and silicate melt: implications for melt

structure and calcium content of magmatic olivines. *Contributions to Mineralogy and Petrology* **136**, 63–80.

MITCHELL, R. H. 1985. A review of the mineralogy of lamproites. *Transactions of the Geological Society of South Africa* **88**, 411–37.

MITCHELL, R. H. 1995. Melting experiments on a sanidine phlogopite lamproite at 4–7 GPa and their bearing on the sources of lamproitic magmas. *Journal of Petrology* **36**, 1455–74.

MITCHELL, R. H. & BERGMAN, S. C. 1991. *Petrology of Lamproites*. New York and London: Plenum Press, 447 pp.

MITCHELL, R. H. & EDGAR, A. D. 2002. Melting experiments on SiO_2-rich lamproites to 6.4 GPa and their bearing on the sources of lamproite magmas. *Mineralogy and Petrology* **74**, 115–28.

MORIMOTO, N. 1989. Nomenclature of pyroxenes. *Canadian Mineralogist* **27**, 143–56.

MURPHY, D. T., COLLERSON, K. D. & KAMBER, B. S. 2002. Lamproites from Gaussberg, Antarctica: possible transition zone melts of Archaean subducted sediments. *Journal of Petrology* **43**, 981–1001.

NELSON, D. R. 1992. Isotopic characteristics of potassic rocks: evidence for the involvement of subducted sediments in magma genesis. *Lithos* **28**, 403–20.

NELSON, D. R., MCCULLOCH, M. T. & SUN, S.-S. 1986. The origins of ultrapotassic rocks as inferred from Sr, Nd and Pb isotopes. *Geochimica et Cosmochimica Acta* **50**, 231–45.

PECCERILLO, A. 1985. Roman comagmatic province (Central Italy): Evidence for subduction related magma genesis. *Geology* **13**, 103–6.

PECCERILLO, A. 1992. Potassic and ultrapotassic rock: Compositional characteristics, petrogenesis, and geological significance. *Episodes* **15**, 243–51.

PECCERILLO, A. 1995. Mafic calc-alkaline to ultrapotassic magmas in central-southern Italy; constraints on evolutionary processes and implications for source composition and conditions of magma generation. In *Proceedings of the Symposium on the Physics and the Chemistry of the Upper Mantle*, pp. 171–89. Rio de Janeiro: Academia Brasileira de Ciencias.

PECCERILLO, A. 1999. Multiple mantle metasomatism in central-southern Italy: geochemical effects, timing and geodynamic implications. *Geology* **27**, 315–18.

PECCERILLO, A. 2003. Plio-Quaternary magmatism in Italy. *Episodes, Journal of International Geoscience* **26**, 222–6.

PECCERILLO, A., POLI, G. & SERRI, G. 1988. Petrogenesis of orenditic and kamafugitic rocks from central Italy. *Canadian Mineralogist* **26**, 45–65.

PRELEVIĆ, D. & FOLEY, S. F. 2007. Accretion of arc-oceanic lithospheric mantle in the Mediterranean: Evidence from extremely high-Mg olivines and Cr-rich spinel inclusions in lamproites. *Earth and Planetary Science Letters* **256**, 120–35.

PRELEVIĆ, D., FOLEY, S. F. & CVETKOVIĆ, V. 2007. A review of petrogenesis of Mediterranean Tertiary lamproites: a perspective from the Serbian ultrapotassic province. In *Cenozoic Volcanism in the Mediterranean Area* (eds L. Beccaluva, G. Banchini & M. Wilson), pp. 113–29. Geological Society of America, Special Paper no. 418.

PRELEVIĆ, D., FOLEY, S. F., ROMER, R. L., CVETKOVIĆ, V. & DOWNES, H. 2005. Tertiary Ultrapotassic Volcanism in Serbia: Constraints on Petrogenesis and Mantle Source Characteristics. *Journal of Petrology* **46**, 1443–87.

ROGERS, N. W. 1992. Potassic magmatism as a key to trace-element enrichment processes in the upper mantle. *Journal of Volcanology and Geothermal Research* **50**, 85–99.

ROGERS, N. W., PARKER, R. J., HAWKESWORTH, R. J. & MARSH, J. S. 1985. The geochemistry of potassic lavas from Vulsini, Central Italy, and implications for mantle enrichment process beneath the Roman region. *Contributions to Mineralogy and Petrology* **90**, 244–57.

SAVAŞÇIN, M. Y. & OYMAN, T. 1998. Tectono–Magmatic Evolution of Alkaline Volcanics at the Kirka–Afyon–Isparta Structural Trend, SW Turkey. *Turkish Journal of Earth Sciences* **7**, 201–14.

SHERATON, J. W. & CUNDARI, A. 1980. Leucitites from Gaussberg, Antarctica. *Contributions to Mineralogy and Petrology* **71**, 417–27.

SUN, S.-S. & MCDONOUGH, W. F. 1989. Chemical and isotopic systematics of oceanic basalts; implications for mantle composition and processes. In *Magmatism in the Ocean Basins Saunders* (eds A. D. Saunders & M. J. Norry), pp. 313–45. Geological Society of London, Special Publication no. 42.

THOMPSON, R. N. 1997. Primary basalts and magma genesis. III. Alban Hills, Roman Comagmatic Province, central Italy. *Contributions to Mineralogy and Petrology* **55**, 1–31.

VENTURELLI, G., CAPEDRI, S., DI BATTISTINI, G., CRAWFORD, A. J., KOGARKO, L. N. & CELESTINI, S. 1984*a*. The ultrapotassic rocks from southeastern Spain. *Lithos* **17**, 37–54.

VENTURELLI, G., THORPE, R. S., DAL PIAZ, G. V., DEL MORO, A. & POTTS, P. J. 1984*b*. Petrogenesis of calc-alkaline, shoshonitic and associated ultrapotassic Oligocene volcanic rocks from the Northwestern Alps, Italy. *Contributions to Mineralogy and Petrology* **86**, 209–20.

WAGNER, C. & VELDE, D. 1986. The mineralogy of K-richterite-bearing lamproites. *American Mineralogist* **71**, 17–37.

ZINDLER, A. & HART, S. 1986. Chemical geodynamics. *Annual Review of Earth and Planetary Sciences* **14**, 493–571.